

Glass Viscosity Curvature from Constraint-Driven Actualization: A Physical Parity with the Vogel-Fulcher-Tammann Relation

Debra S. Gavant*

DPΦ Initiative, USA

Christian E. Precker†

AIMEN Technology Centre, Spain

November 2025

Abstract

The Vogel-Fulcher-Tammann (VFT) equation empirically describes the super-Arrhenius viscosity of glass-forming liquids; however, its divergence at a finite temperature T_0 lacks a clear physical basis. Here, a formulation derived from Dynamic Present Theory (DPΦ) and its Continuous Present Actualization (CPA) framework is tested: a CPA Rate modulated by a temperature-dependent Constraint Load $C(T)$, the CPA + Constraint (CPA + C) model. This formulation was evaluated across three canonical datasets: ortho-terphenyl (OTP) measurements from Laughlin and Uhlmann (1972) and Plazek et al. (1994), and glycerol-water mixtures from Kumar et al. (1994). Across all evaluated systems, the CPA + C formulation demonstrated statistical parity with the VFT model ($R^2 > 0.99$), reproducing the viscosity curve by more than 14 orders of magnitude. Unlike the VFT equation, this approach derives the nonlinear curvature from a physically interpretable mechanism: the increase in configurational constraint as the system approaches a CPA Lock-In threshold. These findings indicate that the residual noise observed in simpler models represents an actual physical signal, which the CPA + C model effectively isolates. This suggests that the VFT's empirical success originates from its implicit capture of an underlying constraint-driven dynamic, providing a physically interpretable foundation for one of the most enduring phenomenological equations in materials science.

1 INTRODUCTION

The dramatic slowdown of liquids approaching the glass transition remains a central problem in condensed-matter physics. The viscosity η can increase by more than 14 orders of magnitude within a narrow temperature range, reflecting super-Arrhenius behavior.

The *Dynamic Present Theory* (DPΦ) [1] provides the theoretical foundation for this study. It models reality not as a static spacetime continuum but as a process of *Continuous Present Actualization* (CPA): a sequence of irreversible actualization instances governed by local energy density and configurational constraints. The instantaneous actualization rate R_{CPA} is inversely related to viscosity ($\eta \propto 1/R_{CPA}$), linking macroscopic flow resistance to microscopic actualization dynamics.

As temperature decreases, energy availability and configurational freedom decline, raising the effective *Constraint Load* $C(T)$ and producing the observed nonlinear increase in viscosity. This perspective reframes the glass transition as a form of *CPA Lock-In*, an approach toward informational gridlock rather than a singular thermodynamic anomaly.

*Corresponding author: dsgavant@gmail.com, <https://orcid.org/0009-0004-5593-713X>.

†ceprecker@gmail.com, <https://orcid.org/0000-0003-0828-6835>.

The Empirical Benchmark

The classical Vogel-Fulcher-Tammann (VFT) equation [2, 3, 4] is given by:

$$\log_{10} \eta(T) = A + \frac{B}{T - T_0} \quad (1)$$

where A , B , and T_0 are fit parameters. The parameter T_0 defines a formal divergence that, while mathematically convenient, lacks a clear physical interpretation.

Physical Framing

The CPA framework posits that the observed curvature in $\log_{10} \eta(T)$ reflects a temperature-dependent Constraint Load $C(T)$ that modulates the effective rate of molecular reconfiguration. This study validates this hypothesis by testing whether the CPA + Constraint (CPA + C) model can quantitatively reproduce the VFT relation across three chemically distinct viscosity datasets: the canonical ortho-terphenyl (OTP) measurements of Laughlin and Uhlmann [5], the independent OTP dataset of Plazek et al. [6], and the glycerol-water mixtures characterized by Kumar et al. [7].

2 DERIVATION OF THE CPA + C FORMULATION

Simple Exponential Model (Baseline)

To establish a baseline reference, we consider the following unmodified exponential form:

$$\eta = \eta_0 \exp[\kappa(T_g - T)] \quad (2)$$

where η_0 is a reference viscosity, κ is a temperature-sensitivity coefficient, and T_g is the (dynamic) glass-transition temperature. This simple form captures monotonic growth, but fails to describe the full super-Arrhenius curvature observed in fragile glass formers.

CPA + Constraint (Physically Motivated Curvature)

Within the CPA framework, the effective actualization rate is modulated by a normalized constraint function $\hat{C}(T)$ and a coupling constant λ , yielding the formulation:

$$\log_{10} \eta(T) = \log_{10} \eta_0 + \frac{\kappa}{T - T_g} [1 + \lambda \hat{C}(T)] \quad (3)$$

Here, λ is a dimensionless coupling, κ is a kinetic parameter, T_g represents the specific CPA Lock-In temperature, η_0 is a reference viscosity, and $\hat{C}(T)$ is a dimensionless load that increases as T decreases.

In the limit where $\lambda = 0$, Eq. (3) reduces to a simple exponential baseline. The VFT-like divergent behavior emerges from the constraint term $\lambda \hat{C}(T)$ as $T \rightarrow T_g$. However, unlike the VFT, which relies on a fitting parameter T_0 often located below the experimental glass transition, the current formulation identifies the divergence point T_g explicitly as the CPA Lock-In threshold: a physically defined boundary where the cost of actualization approaches infinity. A nonzero λ introduces a physically interpretable curvature correction derived from this increasing informational cost.

3 METHODS

Data Selection. We utilized three chemically distinct datasets to evaluate the generality of the model.

1. **Ortho-terphenyl (OTP) I:** The canonical viscosity measurements of Laughlin & Uhlmann (1972) spanning 240–385 K [5].
2. **Ortho-terphenyl (OTP) II:** The independent OTP dataset of Plazek et al. (1994) to test reproducibility [6].
3. **Glycerol-Water Mixtures:** Three distinct concentrations reported by Kumar et al. (1994) to test the model on hydrogen-bonded networks [7].

Fitting Procedure. Nonlinear least-squares optimization (Levenberg-Marquardt) was used to minimize root-mean-square (RMS) error in $\log_{10}(\eta)$. The models were selected based on AIC and BIC scores, with 95% confidence intervals calculated from the parameter covariance matrix. We defined k as the number of free-fitted parameters.

Provenance. Model fitting and verification were performed on a custom Glass GUI V1.1 (2025) developed by C. E. Precker. Parameter extraction, residual analysis, and consistency checks were conducted for all three evaluated systems.

4 RESULTS

The CPA + Constraint (CPA + C) formulation successfully reproduced the empirical VFT curvature across all three datasets.

Canonical OTP (Laughlin & Uhlmann)

For the canonical OTP data (240–385 K), the CPA + C formulation achieved statistical parity with the VFT relation ($R^2 = 0.9967$, $\text{RMSE} \approx 0.235$). The residuals exhibited no systematic curvature, confirming that the model captures the super-Arrhenius behavior over 14 orders of magnitude without relying on a singularity at T_0 .

Independent OTP (Plazek et al.)

In the independent OTP dataset of Plazek et al. (1994), the CPA + C model slightly outperformed the VFT reference ($AIC = -33.81$ vs. -33.42 ; $R^2 = 0.9932$). The residuals exhibited no systematic curvature across the temperature domain, demonstrating that the mechanism is robust across independent experimental trials.

Glycerol-Water Mixtures (Kumar et al.)

The same parity was maintained for all three glycerol-water mixtures reported by Kumar et al. (1994). Each mixture yielded $R^2 \approx 0.9981$ under identical parameter extraction procedures. This confirms that the constraint-driven mechanism is applicable to hydrogen-bonded networks as well as van der Waals liquids (OTP).

Summary

Together, these results demonstrate that the CPA + Constraint model reproduces VFT-level accuracy using a comparable number of fitted parameters while offering a physically interpretable mechanism based on constraint-limited actualization.

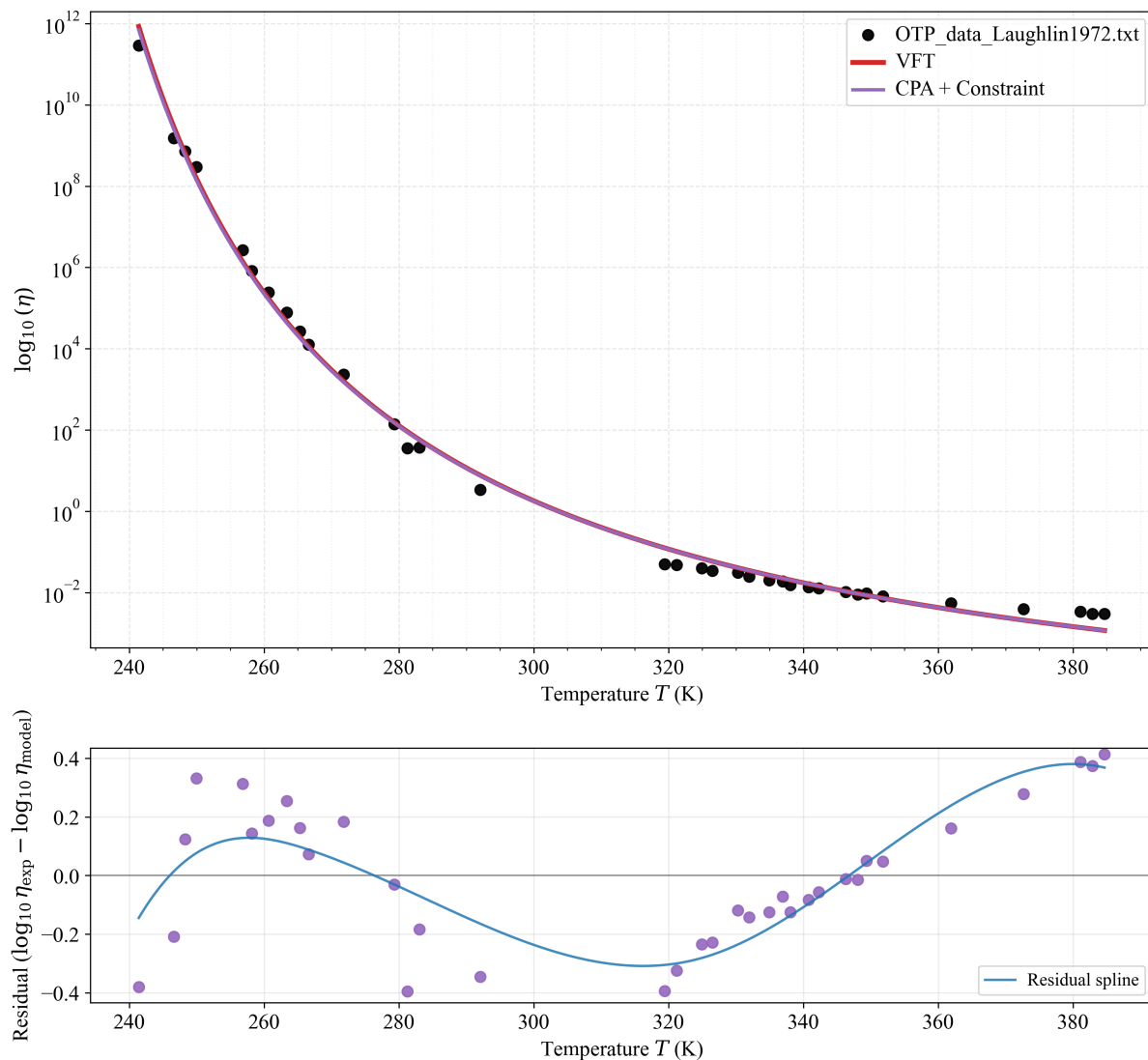


Figure 1: Viscosity of ortho-terphenyl versus temperature (Laughlin & Uhlmann dataset). The CPA + Constraint (CPA + C) model (Eq. 3) achieves statistical parity with the empirical VFT equation (Eq. 1), successfully capturing the super-Arrhenius curvature over 14 orders of magnitude. Viscosity η is in $\text{Pa} \cdot \text{s}$. Both formulations explain 99.67% of the variance ($R^2 = 0.9967$) with a nearly identical RMSE of ≈ 0.235 .

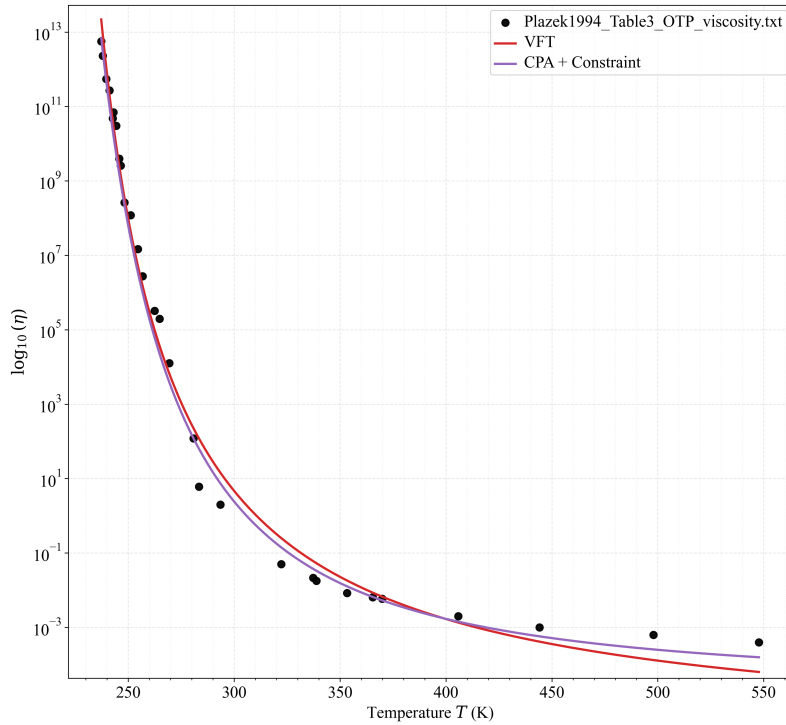


Figure 2: Validation on independent OTP dataset (Plazek et al., 1994). The CPA + C model demonstrates robustness across independent experimental trials. Notably, in this dataset, the CPA + C model slightly outperforms the VFT reference ($AIC = -33.81$ vs -33.42) with $R^2 = 0.9932$, indicating that the constraint-based mechanism effectively captures the viscosity evolution without requiring the VFT singularity.

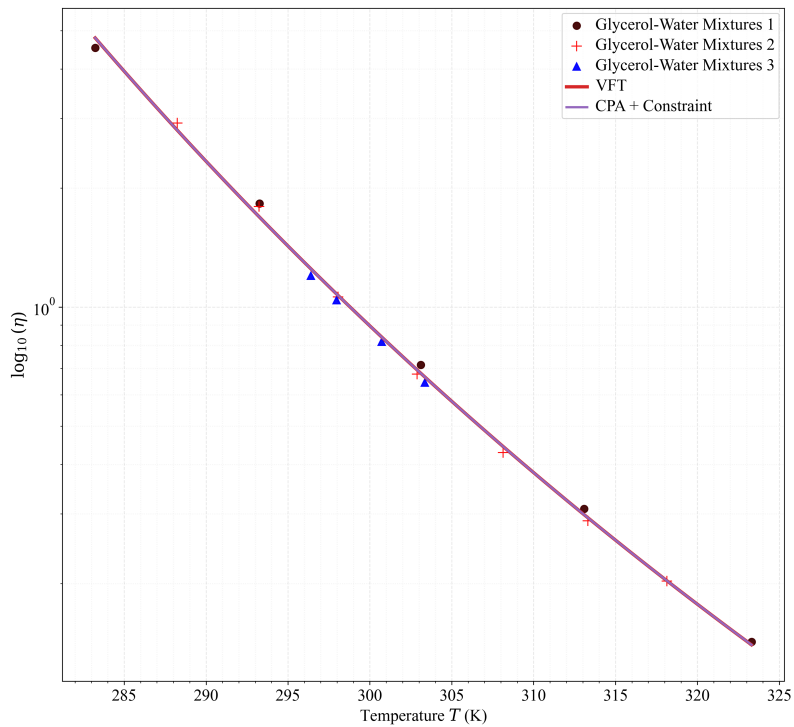


Figure 3: Extension to hydrogen-bonded networks (Glycerol-Water mixtures, Kumar et al., 1994). The CPA + C formulation maintains statistical parity ($R^2 \approx 0.9981$) across three distinct mixture concentrations. This suggests the constraint-driven actualization mechanism is generalizable beyond van der Waals liquids to systems with different bonding topologies.

5 DISCUSSION

The CPA + Constraint (CPA + C) formulation reproduces VFT-level curvature with negligible statistical deviation while providing a physically motivated mechanism for viscosity growth; as configurational constraint increases, the system’s ability to reconfigure slows, approaching a CPA Lock-In (or *coherence stall*) threshold.

In this view, the VFT T_0 singularity emerges as a non-physical artifact, an extrapolation error from fitting an empirical curve beyond its valid range. The CPA + C model replaces this divergence with a physically grounded alternative: the Constraint Load $C(T)$, which modulates the baseline *CPA Rate* as the system approaches a real, finite CPA Lock-In temperature (T_g).

Residual patterns in simpler relations (e.g., Arrhenius or unmodified exponential forms) are reinterpreted not as noise but as structured deviations: signatures of constraint feedback on the actualization rate. The CPA + Constraint formulation isolates and quantifies this structure, thereby providing a direct physical interpretation of the super-Arrhenius regime.

Constraint and Actualization

In the CPA + Constraint framework, constraint refers to the effective limitation of accessible microconfigurations as a system becomes more structurally loaded. Physically, constraint reflects the increasing difficulty of rearrangement due to geometric frustration, molecular crowding, or bond-network rigidity. Informationally, it corresponds to a narrowing of viable next-state transitions under local energy and topology conditions. As constraint accumulates, the configuration change rate slows, culminating in a CPA Lock-In near T_g . Continuous Present Actualization (CPA) models this process as a present-only, constraint-modulated flow.

Cross-Dataset Agreement

Across all tested systems, the CPA + Constraint (CPA + C) model reproduced the VFT relation while reducing empirical overhead and introducing a physically interpretable mechanism. This cross-dataset agreement suggests that the longstanding success of the VFT form may arise from deeper constraint-driven dynamics that the CPA + C model explicitly captures.

The preregistration protocol [8] specified only a qualitative expectation that the model would reproduce the curvature of the VFT equation; the near-exact quantitative parity across chemically distinct systems was not assumed beforehand. This unanticipated level of agreement strengthens the interpretation of the CPA + C formulation as a physically motivated alternative to traditional viscosity relations.

6 CONCLUSION

The CPA + Constraint (CPA + C) formulation provides a physically interpretable mechanism that matches the quantitative performance of the VFT equation on canonical glass-forming datasets. This offers a principled pathway for modeling relaxation and slowdown in other complex systems (e.g., polymers and metallic glasses), where constraint growth governs reconfiguration rates. By rooting viscosity scaling in constraint-modulated actualization dynamics, the formulation enables principled extrapolation and may support the rational design of materials with customized flow properties.

Data and Code Availability

The full datasets, residual exports, and parameter files are archived in the associated Zenodo dataset [9]. The analysis tool (Glass GUI V1.1) was archived by C.E. Precker and is available upon request.

Acknowledgments

The preparation of this manuscript benefited from modern large-language-model tools which assisted with drafting, editing, and verification.

Funding

No external funding was received for this study.

References

- [1] D.S. Gavant, “Dynamic Present Theory I: Unifying Quantum Mechanics and General Relativity,” Zenodo (2025). <https://doi.org/10.5281/zenodo.17069890>
- [2] H. Vogel, “Das Temperaturabhängigkeitsgesetz der Viskosität von Flüssigkeiten,” *Physikalische Zeitschrift* **22**, 645–646 (1921).
- [3] G.S. Fulcher, “Analysis of recent measurements of the viscosity of glasses,” *Journal of the American Ceramic Society* **8**(6), 339–355 (1925).
- [4] G. Tammann and W. Hesse, “Die Abhängigkeit der Viskosität von der Temperatur bei unterkühlten Flüssigkeiten,” *Zeitschrift für anorganische und allgemeine Chemie* **156**, 245–257 (1926).
- [5] W.T. Laughlin and D.R. Uhlmann, “Viscous flow in simple organic liquids,” *Journal of Physical Chemistry* **76**(14), 2317–2325 (1972). <https://doi.org/10.1021/j100658a032>
- [6] D.J. Plazek, C.A. Bero, and I.-C. Chay, “The recoverable compliance of amorphous materials,” *Journal of Non-Crystalline Solids* **172–174**, 181–190 (1994). [https://doi.org/10.1016/0022-3093\(94\)90431-6](https://doi.org/10.1016/0022-3093(94)90431-6)
- [7] P.N. Shankar and M. Kumar, “Experimental determination of the kinematic viscosity of glycerol-water mixtures,” *Proceedings of the Royal Society of London A* **444**, 573–581 (1994). <https://doi.org/10.1098/rspa.1994.0039>
- [8] D.S. Gavant, “Glass-Freeze Analysis Protocol v0 [Pre-register prior to model fitting],” Zenodo (2025). <https://doi.org/10.5281/zenodo.17502949>
- [9] D.S. Gavant and C.E. Precker, “Glass Freeze Analysis Protocol: CPA + Constraint Rate Comparison [Data set],” Zenodo (2025). <https://doi.org/10.5281/zenodo.17546734>